TOWARDS MORE EFFICIENT DRUG DELIVERY: BLOOD FLOW IN STENOTIC ARTERIES SUBJECTED TO A STRONG NON-UNIFORM MAGNETIC FIELD

Saša Kenjereš
Department of Multi Scale Physics, Faculty of Applied Sciences
and J. M. Burgerscentre for Fluid Dynamics,
Deft University of Technology,
Lorentzweg 1, 2628 CJ Delft, The Netherlands
S.Kenjeres@TUDelft.nl

ABSTRACT

The paper reports on a comprehensive mathematical model for simulations of blood-flow under presence of non-uniform magnetic fields. The model consists of from set of Navier-Stokes equations extended with both Lorentz and magnetization forces including a simplified set of Maxwell's equations (Ampere's law) for predictions of imposed magnetic fields. An extensive literature survey is performed in order to find all relevant hydrodynamic and electro-magnetic properties of human blood. The model is then extensively tested for a range of test cases ranging from a simple cylindrical geometries to realistic right-coronary arteries in humans. Both, a time-dependency of the wall-shear-stress for different stenosis growth rates as well as effects of an imposed non-uniform magnetic fields on the blood flow pattern are presented and analyzed. It is concluded that an imposed non-uniform magnetic field can create significant changes in the secondary flow patterns thus making it possible to use this technique for optimized targeted drug delivery.

INTRODUCTION

One of the main problems of a chemotherapy is often not the lack of efficient drugs, but essential inability to deliver precisely and to concentrate these drugs in affected areas. Failure to provide localized targeting results in an increase of toxic effects on neighboring organs and tissues. One promising method to accomplish precise targeting is the magnetic drug delivery. Here, a drug is bound to a magnetic compound injected into the blood stream. The targeted areas are subjected to an external magnetic field that is able to affect the blood stream by reducing its flow rate. In these regions the drug is slowly released from the magnetic carriers. Consequently, relatively small amounts of a drug magnetically targeted to the localized disease site can replace large amounts of the freely circulating drug. At the same time, drug concentrations at targeted site will be significantly higher compared to the ones delivered by standard (systemic) delivery methods. Very encouraging findings have been recently reported in the clinical applications of the magnetic drug targeting including patients with an advanced and unsuccessfully pre-treated cancer or sarcoma, Alexoiu *et al.* (2000,2002,2003).

We belive that numerical simulations can significantly contribute to further advancements of this technique. Since the key to success is associated with the possibility to deliver drugs at particular sites and with precise dosages, personalized parametric numerical studies can be performed - mimicking individual patients conditions. By specifying initial and boundary conditions in mathematical models that include exact size and precise locations of the affected site, it will be possible to design optimized ways of drug delivery for individual patient conditions. Different set of simulations analyzing the optimal diameter of the magnetic particle carriers can lead to optimal solutions for the therapeutic drug preparations. For this purpose, a very first step is to obtain fundamental insights into underlying physics of the blood flow under presence of a strong non-uniform magnetic field. This is primary goal of the presented investigation.

EQUATIONS AND MATHEMATICAL MODEL

Equations describing a laminar incompressible flow of a Newtonian and electrically conducting bio-fluid (blood) subjected to external electro-magnetic fields consist of the combined set of the extended Navier-Stokes and Maxwell equations as follows:

$$\nabla \cdot \mathbf{V} = 0, \quad \nabla \cdot \mathbf{B} = 0 \tag{1}$$

$$\frac{\partial \mathbf{V}}{\partial t} + (\mathbf{V} \cdot \nabla)\,\mathbf{V} = \nu \nabla^2 \mathbf{V} + \frac{1}{\rho}\left[-\nabla P + \underbrace{\mathbf{J} \times \mathbf{B}}_{\mathbf{F^L}} + \underbrace{\mu_0\,(\mathbf{M} \cdot \nabla)\,\mathbf{H}}_{\mathbf{F^M}} \right] \tag{2}$$

$$\nabla \times \mathbf{H} = \mathbf{J}, \quad \nabla \cdot \mathbf{J} = 0, \quad \mathbf{J} = \sigma\,(\mathbf{E} + \mathbf{U} \times \mathbf{B}) \tag{3}$$

where ρ, σ and ν are density, electric conductivity and kinematic viscosity of working fluid. $\mathbf{H}, \mathbf{J}, \mathbf{E}, \mathbf{B}$ are the magnetic field intensity, total electric current, electric field and magnetic induction, respectively.

In the momentum equation (Eq. 2) there are two kinds of body forces caused by imposed electromagnetic fields which act on the bio-magnetic fluid (blood): the Lorentz force ($\mathbf{F^L}$, caused by electric conductivity of the moving fluid through an imposed magnetic field) and the magnetization force ($\mathbf{F^M}$, bio-fluid magnetization response- attraction or repulsion - due to non-uniformity of the imposed magnetic field), Tzirtzilakis (2005). In the blood vessels whose diameters exceed 10^{-4} m blood can be regarded as practically homogeneous because the scales of the microstructures (with typical diameters of $8{\times}10^{-6}$ m for red and white cells and 2-$4{\times}10^{-6}$ m for platelets) are much smaller than that of flow, Pedley (1980). It is generally accepted that blood behaves as a Newtonian fluid at shear rates above 100 s^{-1}, Pedley (1980), Berger and Jou (2000).

However, in the time-dependent studies mimicking an entire cardiac cycle, there are periods of time where the

shear rate is below this 100 s^{-1} limit, implying that the non-Newtonian effects start to be important. In a recent study on simulations of a steady blood flow in coronary arteries, Johnston *et al.* (2004), have compared five different non-Newtonian blood viscosity models (Newtonian, Carreau, Walburn-Schneck, Power Law, Casson and Generalized Power Law models) and found out that the non-Newtonian effects were important only for the low inlet velocities (Re<50). In the follow-up study, addressing now the non-Newtonian effects in transient simulations, same authors concluded that the non-Newtonian model is only significant for approximately 30% of the cardiac cycle, Johnston *et al.* (2006). These periods with non-Newtonian effects have been based on simulations with resting heart rate with relatively low inlet velocities - so these periods will be significantly reduced with further elevation of the heart rate. In this study, we will use a Newtonian viscosity based blood model that represents a good first approximation for practical applications since our primary target is to focus on a magnetic field effects. The simulations using more advanced non-Newtonian models are currently under development and will be reported in a later publication.

Under the assumption that the magnetization ($\mathbf{M}$) and the magnetic field ($\mathbf{H}$) are parallel, the magnetization force can be written as $\mathbf{F^M} = \mu_0 M \nabla H$, where $M = |\mathbf{M}|$ and $H = |\mathbf{H}|$. The intensity of magnetization in a bio-fluid generally depends on its temperature and density as well as on the magnetic field intensity. Accordingly, different magnetization models are proposed in literature in order to take into account these parameters. The most elaborate mathematical model of the magnetization is expressed by the Langevian function, $L(\xi)$:

$$M = n \cdot m \cdot L(\xi) = n \cdot m \left(coth\ \xi - \frac{1}{\xi} \right), \quad \xi = \frac{\mu_0 m H}{\kappa T} \tag{4}$$

where n, m, κ, T are number of particles per unit volume, magnetic moment of a particle, Boltzmann constant and absolute temperature, respectively, Berkovsky *et al.* (1993), Odenbach (2002). Here, we adopted a simplified model for the magnetization since the considered problem does not involve any temperature changes (isothermal conditions):

$$M = \chi H \tag{5}$$

where χ is the magnetic susceptibility, Berkovsky *et al.* (1993), Rosensweig (1997). It is experimentally determined that in the presence of the static magnetic fields the magnetic susceptibility of blood strongly depends of its local conditions, i.e. oxygenated blood behaves as a diamagnetic ($\chi^{\mathsf{oxyg}} = -6.6 \times 10^7$) and de-oxygenated blood behaves as a paramagnetic ($\chi^{\mathsf{deoxyg}} = 3.5 \times 10^{-6}$) material, Haik *et al.* (1999). The change in magnetic susceptibility for de-oxygenated and oxygenated blood is caused by the binding of oxygen to the blood protein hemoglobin, which is responsible for transport of oxygen within a human body.

Similarly, the electrical conductivity of blood in animals and humans (in contrast to remaining tissues of a body) has a significant value and the effects of Lorentz force caused by blood stream through an imposed magnetic field should be taken into account. Experiments presented in literature demonstrated that the electrical conductivity of blood depends on the underlying velocity of the blood stream, i.e. the electrical conductivity of moving blood is higher than from the stationary one, Hoetink *et al.* (2004), Balan *et al.* (2004). This increase of the electrical conductivity is caused by reorientation of erythrocytes (red blood cells, RBC) influenced by the viscous forces, Fujii *et al.* (1999). Visser (1989) experimentally determined that compared to the stationary blood, the electrical conductivity of the flowing blood increased by 10, 15 and 20% (averaged) for the packed cell values (or hematrocit) of 36.4, 47.5 and 53.7%, respectively. The measured electrical conductivity of flowing blood were in $0.7 \leq \sigma \leq 0.9$ range.

Table 1: Properties of the bio-magnetic fluid (blood) used for numerical simulations.

ρ	ν	σ	χ^{oxyg}	χ^{deoxyg}
1050.	4×10^{-6}	$0.7 - 0.9$	-6.6×10^{-7}	3.5×10^{-6}

When a magnetic field is applied on the flowing blood, additional reorientation of erythrocytes takes place. Higashi *et al.* (1993) found that the erythrocytes are oriented with their disk plane parallel to the magnetic field direction while outside the magnetic field they show no particular orientation. As results of this reorientation the viscosity of blood changes. Haik *et al.* (2001) experimentally determined that blood flow rate decreased by 30% when subjected to a high magnetic field of 10 T. They connected this decrease in the blood flow rate with an increase in the apparent viscosity caused by applied magnetic field. A qualitative interpretation is provided in terms of the apparent viscosity (μ^*) as $\mu^*/\mu \propto L^4(\xi)/\xi^{1/7}$ due to magnetic torques exerted on the the erythrocytes. In present study, we used the values of the apparent viscosity increase as proposed by Haik *et al.* (2001). A short summary of all blood properties is given in Tab.1.

In addition to all blood properties and magnetization force, the Lorentz force should be calculated too. In this work we solved a simplified set of Maxwell's equations by solving a single equation for the electric potential (inductionless assumption). In order to impose magnetic field distributions, a simple Ampere's law is used for the generated magnetic field around series of infinitely long straight wires:

$$B = \frac{\mu_0 I}{2\pi R} \rightarrow B_x = -\mu_0 \sum_{i=1}^{N} \frac{I_i \left(y - y_i^c\right)}{\left(x - x_i^c\right)^2 + \left(y - y_i^c\right)^2},$$
$$B_y = \mu_0 \sum_{i=1}^{N} \frac{I_i \left(x - x_i^c\right)}{\left(x - x_i^c\right)^2 + \left(y - y_i^c\right)^2} \tag{6}$$

Then, a modulus of magnetic field intensity is calculated as:

$$B(x,y,z) = \sqrt{B_x^2 + B_y^2 + B_z^2} \tag{7}$$

where N is number of wires R is distance from the wire center, I is current intensity and μ_0 is the magnetic permeability in vacuum ($4\pi \cdot 10^{-7}$)

NUMERICAL METHOD

The equation set is solved using an in-house finite volume solver for three-dimensional flows in structured non-orthogonal geometries. The parallel execution is based on the domain-decomposition technique utilizing MPI directives. The Cartesian vectors and tensors components in collocated grid arrangement are applied for all variables. The second-order QUICK scheme is applied for discretization of convective terms in momentum equations. The second-order central difference scheme is applied for diffusive terms. The fully implicit time integration based on three-consecutive time steps values is used for the time-dependent terms.

RESULTS AND DISCUSSION OF NUMERICAL SIMULATIONS

Steady blood flow through a cylinder subjected to non-uniform magnetic fields

In order to validate implementation of the extended set of the Navier-Stokes equations with additional electromagnetic forcing and to demonstrate principles behind fluid flow reorganization, a simplified flow through an infinitely long pipe with a diameter corresponding to a typical artery size (Re=500) are considered first, Fig. 1. The numerical mesh in the vertical plane consisted of 82×82 CVs strongly clustered in the near-wall region. Different configurations of imposed magnetic field are analyzed for both de-oxygenated and oxygenated blood. A characteristic situation with a magnetic field created from a single current carrying wire located in the central vertical plane at a distance of 5 mm from the blood vessel wall. Under influence of an uniformly distributed (in the vertical direction) strong magnetic field ($|B|$=10 T) flow is just slightly affected by underlying

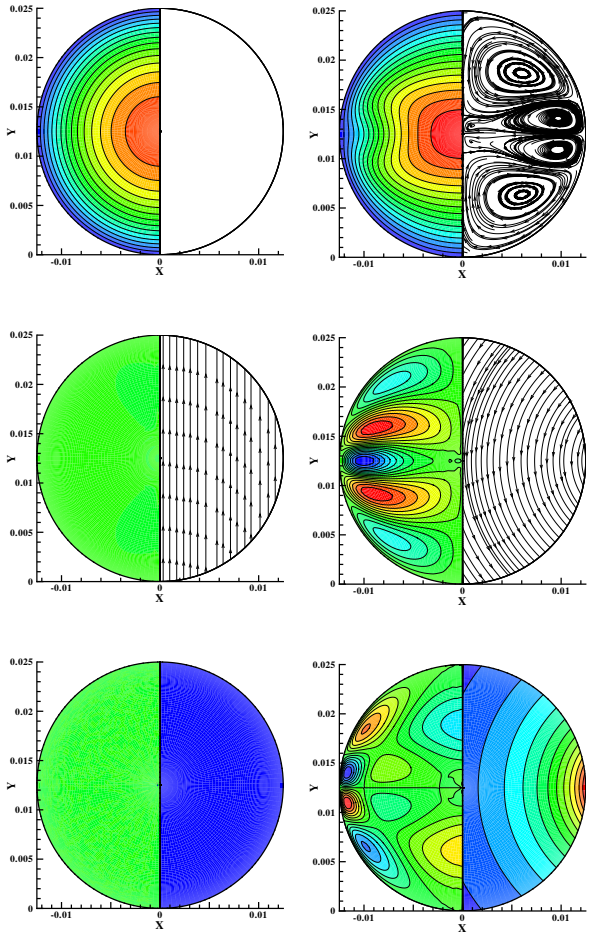

Figure 1: De-oxygenated blood flow reorganization under influence of an imposed non-uniform magnetic field, Re=500, B=10 T. First row- contours of the streamwise velocity (W) and streamlines of secondary flow; Second row- contours of the horizontal velocity (U) and magnetic flux lines; Third-contours of vertical velocity (V) and of magnetic field magnitude. Left- uniform vertically oriented magnetic field, Right- a wire source located in the central vertical plane 5 mm from the cylinder wall.

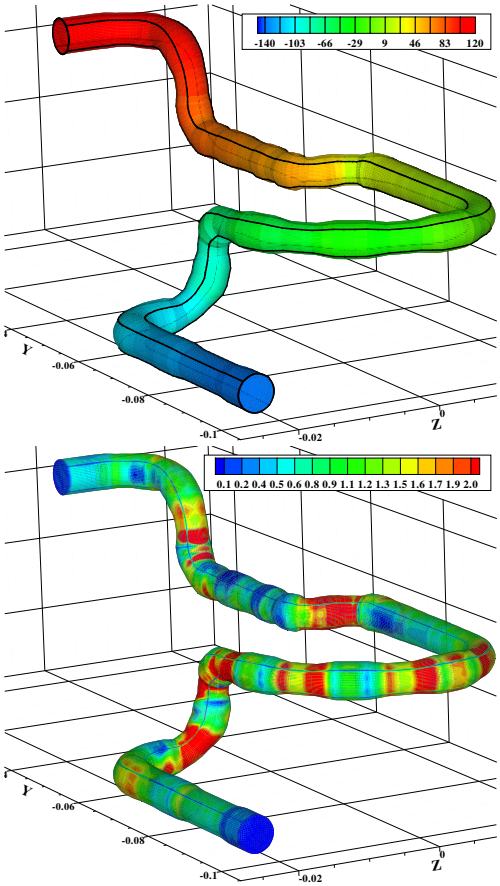

Figure 2: Above- a model of a healthy right-coronary artery; Middle- local pressure distributions; Below- wall shear stress (WSS) distributions (in Pa); Re=500.

Lorentz force since the magnetization force is equal to zero, Fig. 1-left. This situation dramatically changes when non-uniform magnetic field distributions are imposed. Now, the magnetization force takes over Lorentz force and strong secondary motions are generated, Fig. 1-right. Also imprints in streamwise velocity contours are clearly visible. It is important to note that these effects are significantly smaller for oxygenated blood since the magnetic susceptibility is smaller than for the de-oxygenated state (not shown here). It can be concluded that we demonstrated that non-uniformly imposed magnetic fields can have a significant effect on the flow of de-oxygenated blood and that magnetization force effects play a dominant role in flow reorganization.

Pulsating flow in arteries with different stenosis growth rates

Next, we move to a realistic model of a right-coronary artery with different stenosis growth rates. The numerical mesh is created in order to mimic closely the X-ray angiograms presented in Johnston *et al.* (2004,2006) (similar artery diameters and arc-lengths are selected) and consists from 38^2×236 CVs, Figs.2,3. Different stenosis growth rates are created to occupy from 0 to 75 % of the aorta cross-section. These growth rates are indicated as phase0,..., phase3, where phase0 corresponds to healthy and phase3 to 75% clothed artery at stenosis location. A separate simulation is performed in order to obtain fully developed velocity profile at the inlet (with starting uniform distribution of 0.1 m/s). Then in order to mimic realistic pulsating cycle, this fully developed profile is multiplied with a time varying forcing function. This function is obtained from recorded

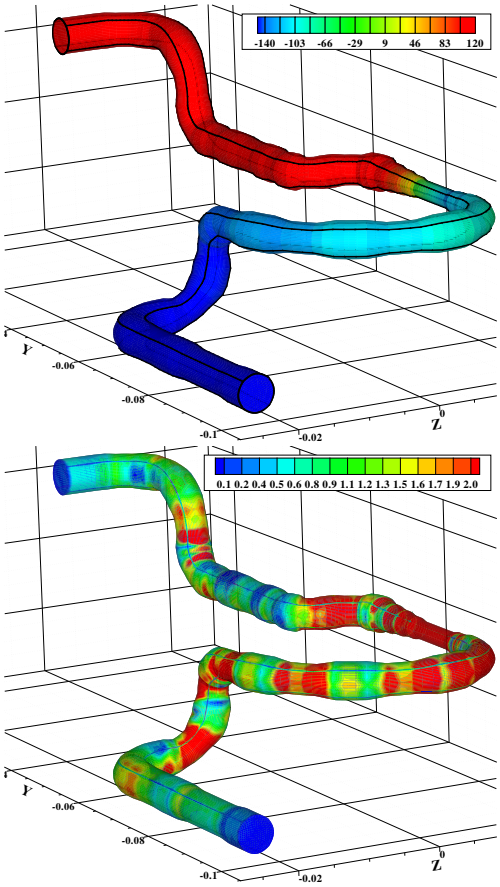

Figure 3: Caption as in previous figure only now for a model of the right-coronary artery with a stenosis reducing 50% of the effective cross-section surface area;

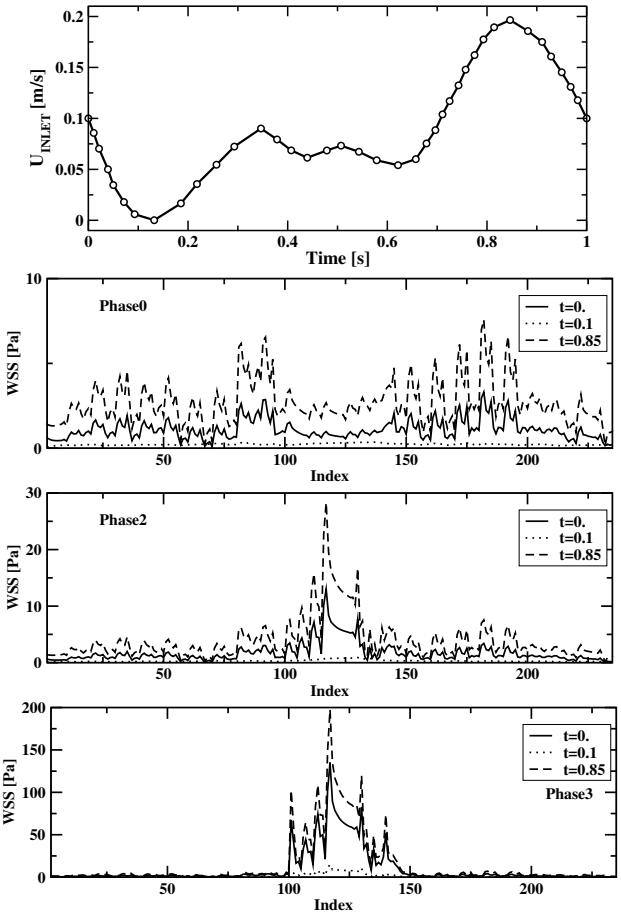

Figure 4: Above- the inlet velocity time-dependency closely mimicking recorded velocity signal in the right-coronary artery of a real patient, Matsuo *et al.* (1988). Below- time dependency of the wall-shear-stress (WSS) distributions along the artery walls for different stages of the stenosis growth (0%, 50% and 75%) respectively.

velocity signals in the right coronary artery of a normal 56 year old female and is presented in work of Matsuo *et al.* (1988), Fig. 4-above. It can be seen that the velocity signal exhibits cycles of strong acceleration and deceleration with characteristic maximal peak of 0.2 m/s at 0.85 sec and almost fully stagnant flow at 0.16 sec. Instantaneous distributions (at 1 sec) of pressure and wall-shear-stress (WSS) along the artery walls for different stenosis growth rates are shown in Figs. 2,3. It is important to report that results are shown for a fully developed pulsating flow regimes, i.e. it was necessary to perform at least 5 cycles in order to get flow fields independent from the initial velocity input profile. It can be seen that the stenosis drastically changes both local flow pattern and pressure distributions and consequently wall-shear-stress distributions along the artery wall. The maximum of the WSS at the peak point (0.85 sec) compared with neutral case (healthy artery) show an increase of factor 5 to 40 for 50% and 75% stenosis growth rates, respectively, Fig. 4. This fact can illustrate strongly increasing risks in the latter stage of the stenosis growth where a relatively small increase of stenosis area can lead to critical rapture of the artery walls.

The velocity vectors in a plane crossing the stenosis location for maximal (0.85 sec) and minimal (0.16 sec) peaks during the pulsating cycle for neutral case and for case with 50% stenosis growth rate are shown in Figs. 5,6. These figures nicely illustrate richness of flow patterns despite laminar flow regime. Regions with strong flow acceleration, decelerations, stagnant zones, recirculation, inner jets, strong reversals, 3D helical patterns- all simultaneously co-exist during a pulsating cycle. It can be seen that the stenosed artery shows more intensive flow velocity caused by reduction in characteristic artery diameter. This intensive jet-like flow changes recirculative pattern downstream of the stenosis location - especially during the maximum peak in pulsating cycle.

After performing these preliminary simulations and after verifying range of obtained WSS values during pulsating cycles - that all were in good agreement with similar results presented in Johnston *et al.* (2004,2006) - new set of simulations is performed with imposed magnetic fields. Both Lorentz and magnetization force are activated and taken into account during these calculations. Also corrections of the blood apparent viscosity in magnetic fields are taken into account in accordance with correlations of Haik *et al.*(2001). The spatial distributions of magnetic field components (B_x and B_z) are shown in Fig. 7. It can be seen that the magnetic field is localized on such way that the potential stenosed region will be influenced most effectively. The comparison between pressure fields for neutral and situation with imposed magnetic field is shown in Fig. 8. It can be seen that a significant local pressure changes are present at locations with significant magnitude of imposed magnetic field. In order to better illustrate a local flow pattern changes caused by imposed magnetic field, vertical cross-sections are plotted with velocity vectors illustrating secondary flow pattern, Fig. 9. For both intersections (lo-

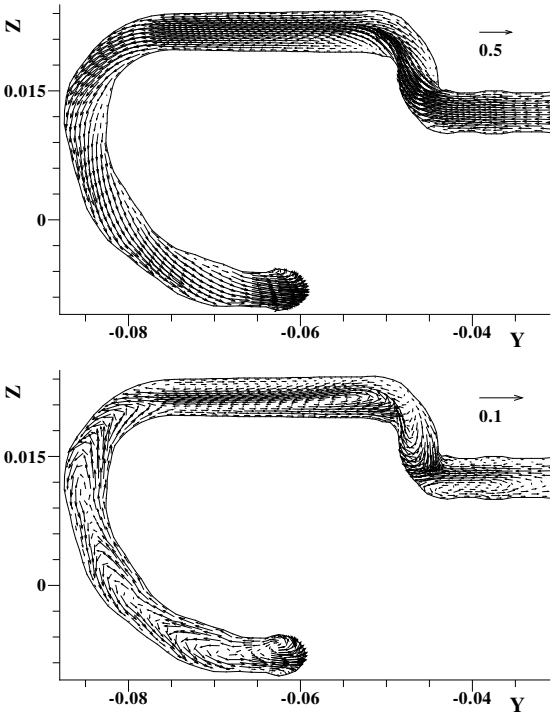

Figure 5: The velocity vectors in a plane crossing the stenosis location for maximal and minimal peaks in flow cycles (0.85 and 0.16 sec) - healthy aorta.

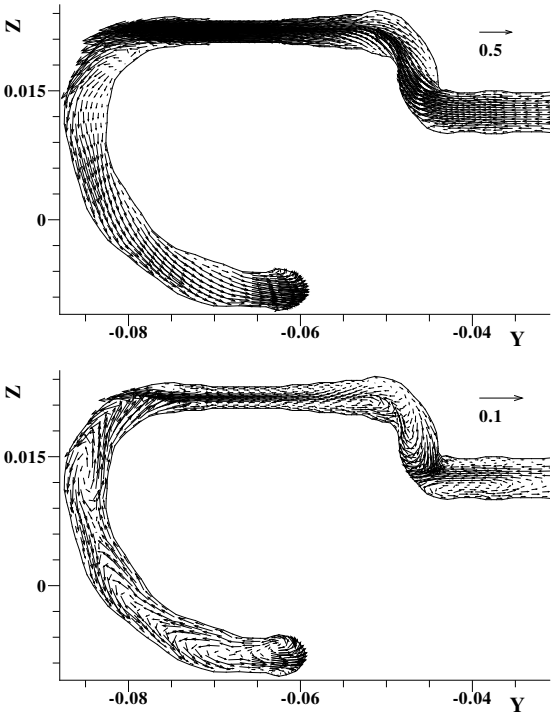

Figure 6: Same as caption in previous figure but now for 50% stenosis growth rate.

cated inside potential stenosed artery segments) significant changes in the flow pattern can be observed. Significantly more intensive secondary motions are observed at both locations when magnetic effects are activated. It confirms our previous conclusions in simplified geometries, i.e. that imposed non-uniform magnetic fields can significantly effect and alter blood-flow patterns at specific locations. This additionally opens a possibility to use a magnetic particles as

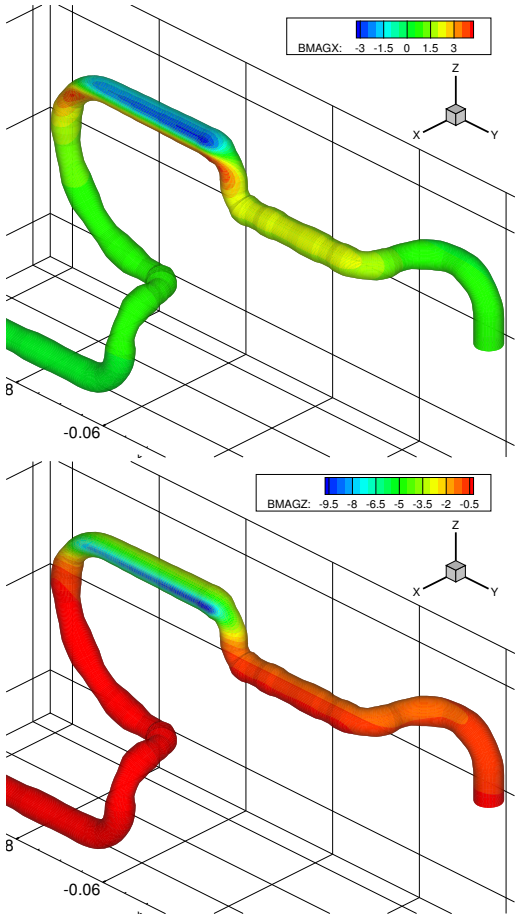

Figure 7: Distribution of a locally imposed magnetic field for a right coronary artery - B_x - above, B_z - below.

a drug carriers that can be locally targeted to diseased regions. In such case, significantly weaker magnetic fields can be used since the magnetization properties of particles can be designed to be few order of magnitude more efficient than these of a normal de-oxygenated blood. The blood flow simulations with magnetic particles will be subject of our future investigations.

CONCLUSIONS

We presented a comprehensive mathematical model for description of blood flow in presence of a strong non-uniform magnetic field. Both, the Lorentz and magnetization forces are taken into account in momentum equations. A simplified set of Maxwell's equations (Ampere's law) is used to calculate imposed magnetic field distributions. An extensive literature survey is performed in order to collect and to model hydrodynamic and magneto-electrical blood properties. The potentials of using a magnetic field to directly influence blood behavior are investigated in details. First a steady blood flow in simplified (a straight pipe) geometry under influence of different locally imposed magnetic fields are performed. It is demonstrated that a very significant flow reorganization takes place when de-oxygenated blood is used as a working fluid. Then a model of a realistic right coronary artery with pulsating flow conditions is simulated. The inlet velocity forcing function is based on realistic measurements performed in a healthy patient. Different scenarios with stenosis growth-rates are simulated and local distributions of pressure and wall-shear-stress along the artery walls are analyzed and compared. Finally, the locally imposed

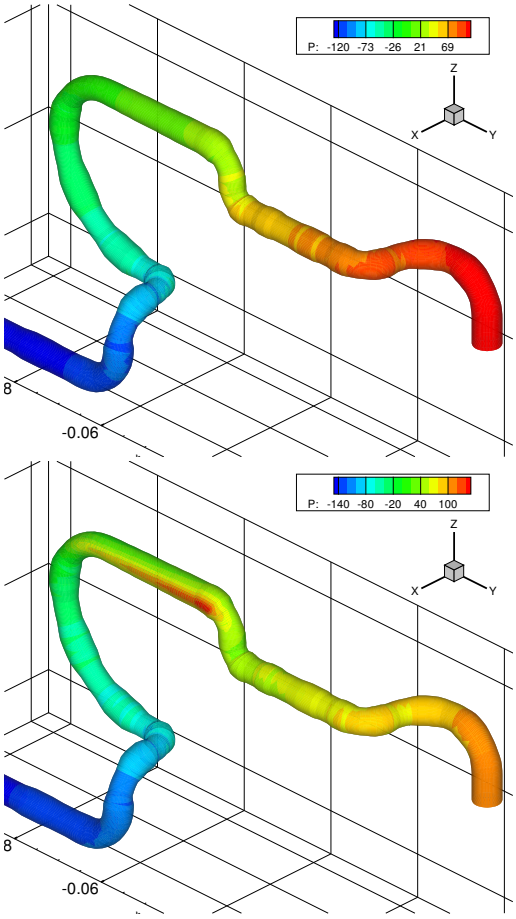

Figure 8: Pressure distributions for a healthy artery without (-above) and with locally imposed magnetic field (-below) both at the end of pulsating cycle (1 sec).

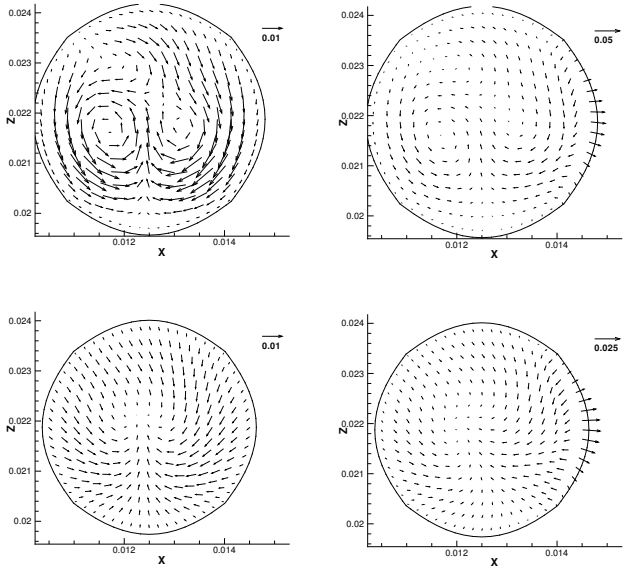

Figure 9: Secondary flow patterns in characteristic planes (middle of stenosis location and 1 cm downstream from the stenosis center) without and with imposed magnetic field of a healthy aorta at the end of the pulsating cycle (1 sec).

magnetic fields are used in realistic artery and proved that local blood-flow pattern is significantly affected by magnetization force.

REFERENCES

Alexiou C. *et al.*, 2000, "Loco-regional Cancer Treatment with Magnetic Drug Targeting", *Cancer Research* **60** (23), pp.6641-6648.

Alexiou C. *et al.*, 2002, "Enrichment and Biodistribution of a Magnetically targeted Drug Carrier", *European Cells and Materials* **3** (2), pp.135-137.

Alexiou C. *et al.*, 2003, "Magnetic drug targeting-biodistribution of the magnetic carrier and the chemotherapeutic agent mitoxantrone after locoregional cancer treatment", *J. Drug Target.* **11** (3), pp.139-149.

Balan C. *et al.*, 2004, "Experimental determination of blood permittivity and conductivity in simple shear flow", *Clinical Hemorheology and Microcirculation* **30**, pp.359-364

Berger S. A. and Jou L. D., 2000, "Flows in stenotic vessels", *Annual Review of Fluid Mechanics* **32**, pp.347-382

Berkovsky B.M., Medvedev V. F. and Krakov M. S., 1993, *Magnetic Fluids: Engineering Applications*, Oxford University Press

Fujii M. *et al.*, 1999, "Orientation and deformation of erythrocytes in flowing blood", *Annals of N.Y. Acad. Sci.* **873**, pp.245-261

Haik Y., Pai V., Chen C.-J., 1999, "Biomagnetic fluid dynamics", in *Fluid Dynamics at Interfaces*, pp. 439-452, eds. W. Shyy and R. Narayanam, Cambridge University Press, Cambridge

Haik Y., Pai V., Chen C.-J., 2001, "Apparent viscosity of human blood in a high static magnetic field", *Journal of Magnetism and Magnetic Materials* **225**, pp. 180-186

Higashi T. *et al.* 1993, "Orientation of Erythrocytes in a Strong Static Magnetic Field", *Blood* **82** (4), pp.1328-1334

Hoetink A. E .*et al.*, 2004, "On the Flow Dependency of the Electrical Conductivity of Blood", *IEEE Transactions on Biomedical Engineering*, Vol.51, No.7, pp.1251-1261

Johnston B.M., Johnston P.R., Corney S., Kilpatrick D., 2004, "Non-Newtonian blood flow in human right coronary arteries: steady state simulations", *Journal of Biomechanics* **37**, pp.709-720

Johnston B.M., Johnston P.R., Corney S., Kilpatrick D., 2006, "Non-Newtonian blood flow in human right coronary arteries: Transient simulations", *Journal of Biomechanics* **39**, pp.1116-1128

Matsuo S. *et al.*, 1988, "Phasic Coronary Artery Flow Velocity Determined by Doppler Flowmeter Catheter in Aortic Stenosis and Aortic Regurgitation", *The Americal Journal of Cardiology*, Vol.62, pp.917-922.

Odenbach S. (Ed.), 2002, *Ferrofluids: Magnetically Controllable Fluids and Their Applications*, Lecture Notes in Physics, Springer-Verlag, Berlin-Heidelberg

Pedley T. J., 1980, *The Fluid Mechanics of Large Blood Vessels*, Cambridge University Press, Cambridge.

Rosensweig R.E.(1997), *Ferrohydrodynamics*, Dover, Mineola, New York (1997).

Tzirtzilakis E.E., 2005, "A mathematical model for blood flow in magnetic field", *Physics of Fluids* **17**, 077103

Visser K. R., 1989, "Electric conductivity of stationary and flowing human blood at low frequencies", *11th Annual International Conference on IEEE Engineering in Medicine and Biology Society*, pp.1540-1542